

Nilogen Oncosystem's High Content Imaging Analysis

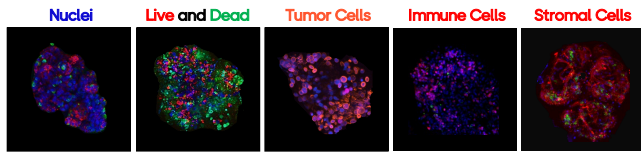


Figure 1: Tumor cell killing analysis scheme using high-throughput 3D confocal imaging to obtain individual-cell data. The process includes identifying cell size, shape, and type using fluorescent labels, determining cell viability or apoptosis, and applying customized staining for specific cell populations. This method enhances analysis precision by evaluating responses at the single-cell level, in contrast to traditional methods that focus on larger-scale responses, like organoid size. It is effective for analyzing small cell numbers and complex tissue structures, addressing limitations of conventional approaches.

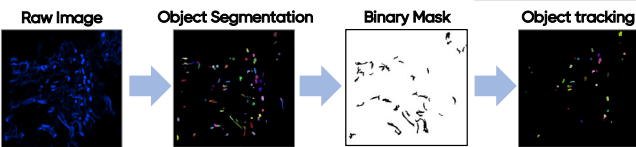


Figure 2: Tumor cell killing image data is pre-processed to exclude non-cellular components from analysis. A specialized segmentation sequence is used to detect irregular fluorescent objects or those with atypical intensity, such as auto fluorescent fibers. This non-cellular mask ensures only cellular objects are included in the final analysis.

Nilogen Oncosystem's Tumor Cell Killing Assay Readout

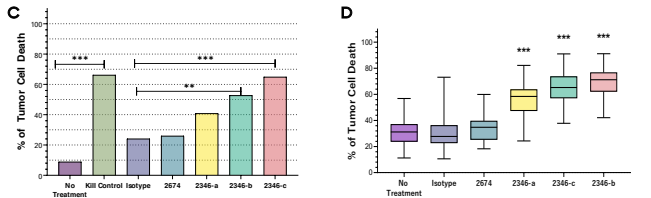
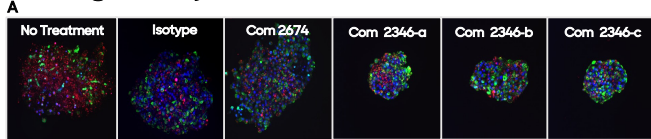


Figure 3: Tumor cell killing data from high-throughput 3D confocal imaging and analysis, capturing tens to hundreds of thousands of data points per sample. Tumoroids treated with negative controls and increasing doses of an oncologic compound show increased dead (green) and decreased live (red) signals with higher doses. Tumor cell killing is quantified as the percentage of cells killed per treatment, visualized through heat maps. (A) Reducing low (green) to high (red) cell killing, and box-and-whisker plots for site average (C) and variance (D) for assessing treatment response variability.

Therapeutic Kill Curve & Dose Kinetics

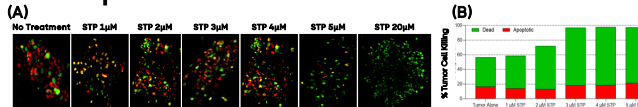


Figure 4: Fluorescent images (A) show tumor cell viability and apoptosis following treatment with increasing concentrations of STP (1.2-20 µM). Green staining indicates apoptotic cells, while red staining marks live cells. As the concentration of STP increases, the proportion of red cells decreases, indicating higher levels of cell death, particularly at 5 µM and 20 µM. The bar graph (B) quantifies the percentage of dead (green) and apoptotic (red) cells across treatments. Higher STP concentrations lead to an increase in tumor cell killing, with the most significant effect observed at 5 µM and above.

Evaluating Mechanism of Tumor Cell Death

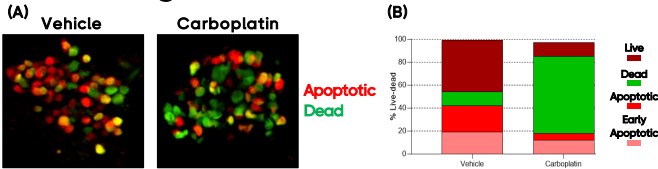


Figure 5: Tumor Cell Viability Following Carboplatin Treatment. (A) Fluorescent images of tumor cells treated with Vehicle (left) and Carboplatin (right). (B) Stacked bar graph quantifying the percentage of live (green) and dead (red) cells in both conditions. Carboplatin treatment significantly increases the percentage of dead cells compared to the vehicle control, highlighting its effectiveness in inducing tumor cell death.

Tumoroid Fragmentation Analysis

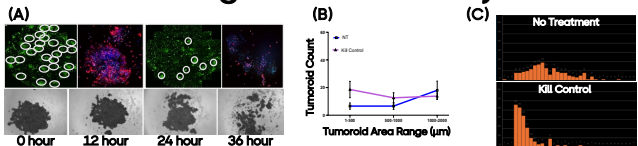


Figure 6: Tumoroid Fragmentation Analysis Following Treatment: (A) Fluorescence and brightfield images of tumoroids over time, showing tumor fragmentation upon treatment. The top row includes fluorescent images of tumoroids with nuclei (blue), apoptotic cells (red), and viability markers (green). (B) Compares the degree of fragmentation over time in treated versus control groups. Significant increases in fragmentation are observed in kill control treated samples (purple line) compared to no treatment (blue line). (C) Histograms quantify tumoroid size distribution reflecting increased cell death and disintegration.

Immune Checkpoint Inhibitor

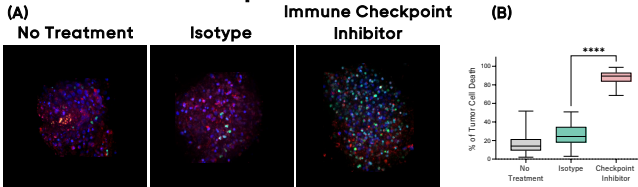


Figure 7: (A) Fluorescent images of tumoroids treated with media, isotype control, and immune checkpoint inhibitor. Blue: nuclei (DAPI), green: apoptotic cells, red: viable cells. The immune checkpoint inhibitor treatment shows increased tumor cell death. (B) The box plot quantifies tumor cell death (%), showing significantly higher death in the immune checkpoint inhibitor group. **** $p < 0.0001$.

Antibody Drug Conjugates

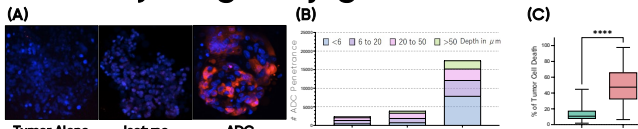


Figure 8: ADC-Mediated Tumor Cell Killing in 3D Tumoroids. (A) Immunofluorescence images show increased targeted cells (red) in ADC-treated tumoroids compared to controls. (B) Quantification of cell penetration shows ADC-treated tumoroids with higher positive cell counts across all depths compared to tumor-alone and isotype controls. (C) Box plot shows significantly increased tumor cell death with ADC treatment.

Virus-based Therapies

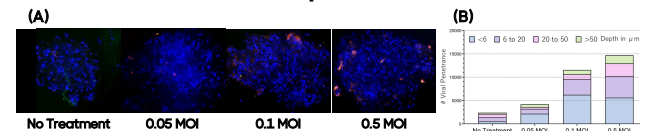


Figure 9: Viral Penetration in Tumoroids. (A) Immunofluorescence images show increased viral penetration (red) in tumoroids greater MOIs (0.05, 0.1, 0.5), especially at 0.5 MOI. (B) Graph quantifies viral penetration by depth, showing deeper and greater penetration at higher MOI, with 0.5 MOI having the most extensive spread.

Bispecific Binding and Infiltration

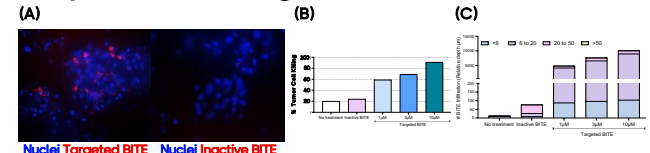


Figure 10: (A) Fluorescent images show nuclei (blue) with BITE staining (red) for Targeted BITE (left) and Nonspecific BITE (right). Targeted BITE shows stronger tumor engagement. (B) Bar graphs quantify tumor cell death, showing higher immune activation with targeted BITE compared to Nonspecific BITE. (C) Indicating greater binding and infiltration.

Cell Therapy

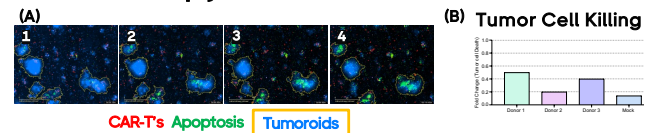


Figure 11: Time-Lapse Imaging of Tumoroids Co-Cultured with CAR-T Cells for Tumor Cell Killing. (A) This figure shows a time-lapse imaging of tumoroids treated with CAR-T cells (red), targeting and killing tumor cells. Imaging every 2 hours tracks CAR-T movement, clustering, and interaction with tumoroids. Over time, apoptotic cells (green) increase, indicating CAR-T-mediated tumor killing, especially in areas with high CAR-T infiltration. (B) The bar graph quantifies tumor cell killing across samples, highlighting CAR-T effectiveness from different donors.

Stromal Targeting Agents and CAR-T Cell Infiltration

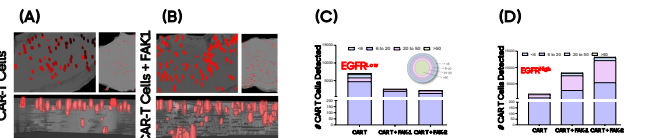


Figure 12: CAR-T Cell Infiltration and Penetration in EGFR⁺ and EGFR⁻ Tumoroids with or without FAK Inhibition. (A) 3D renderings illustrate CAR-T cell infiltration (red) in tumoroids. FAK inhibition (B) enhances infiltration in both EGFR⁺ and EGFR⁻ tumoroids, especially at deeper layers. (C, D) Quantification shows FAK inhibition increases CAR-T cell penetration in tumoroids, with greater penetration observed in EGFR⁻ tumoroids.